Lasers in Manufacturing Conference 2019

Experimental results and modelling of element loss in continuous laser beam welding of aluminum alloys

Florian Hugger[a*], Eric Punzel[a], Michael Schmidt[b,c]

[a]*BBW Lasertechnik GmbH, Gewerbering 11, 83134 Prutting, Germany*
[b]*Institute of Photonic Technologies, Konrad-Zuse-Straße 3/5, 91052 Erlangen, Germany*
[c]*Erlangen Graduate School in Advanced Optical Technologies (SAOT), Paul-Gordan-Str. 6, 91052 Erlangen, Germany*

Abstract

In aluminum alloys the elements magnesium and zinc have a much lower evaporation temperature than the base element. This leads to selective evaporation and loss of these elements in the fusion zone. Moreover, the evaporation rate of volatile elements is determined by a combined process of evaporation and diffusion of these elements from the melt pool towards the capillary surface.
In this paper the influence of welding parameters like feed rate, laser power, focal diameter as well as alloying element concentration on volatile element loss and evaporation rate is investigated. Measuring the keyhole and weld pool geometry, the interaction time of the melt with the laser beam can be calculated. Combining results from element loss and interaction time the diffusion rate of volatile elements towards the keyhole surface is estimated. The evaporation rate of volatile elements is invers proportional to interaction time.

Keywords: Aluminum; laser beam welding; element loss; diffusion; vaporazation

1. Element loss in aluminum alloys

The differences of evaporation temperatures of base material and alloy elements results in selective evaporation. When the evaporation temperature of the alloying elements is significantly lower than the evaporation temperature of the base material, the element is lost during the laser welding process (Mundra

* Corresponding author. Tel.: +49-8036-90-820-65; fax: +49-8036-90-820-28 .
E-mail address: f.hugger@bbw-lasertechnik.de .

and Debroy, 1993). Existing models describe the evaporation process and the transportation mechanisms of alloying elements from the fusion zone towards the surface of the vapor capillary (Dilthey et al., 2001). The two processes are interconnected as the alloying element concentration at the surface is the driving force of the diffusion process in the melt pool. Conversely, the diffusion rate controls the evaporation rate.

There has been studies on the effect of process parameters on element loss which include the influence of alloying element content w (Collur et al., 1987), feed rate v_V (Dilthey et al., 2001), laser power P_L (Liu et al., 2017), pulse duration t_P (Jandaghi et al., 2009) and shielding gas flow rate (Khan et al., 1988). Though the main influencing factors are established, the is no simple model available which provides the potential to estimate the element losses for a given parameter set. For this reason, in the paper a simple calculation procedure is presented to predict the evaporation rate by measurements of the weld seam geometry. The calculations are compared to experimental results. The experimental setup is described in the next section.

2. Experimental procedure

The welding experiments are carried out using a 6-kW disk laser TruDisk 6001 with a scanning optic PFO33. The laser beam is focused to spot diameter d_F of 170 µm at the surface. To investigate the influence of different spot sizes the laser beam is defocused to spot sizes on the surface of 340 µm, 510 µm and 680 µm. The element loss is studied using different aluminum alloys with 2 mm thickness. In every parameter set the sheets are fully penetrated. The alloys and the respective content of volatile elements magnesium and zinc are given in table 1.

Table 1. Alloys and alloying element content of volatile elements measured by WDX.

Alloy	Mg-content x_{Mg}	Zn-content x_{Zn}
AlMg1 (EN AW-6082)	0.75 wt%	0.1 wt%
AlMg3 (EN AW-5457)	2.79 wt%	0.1 wt%
AlMg5 (EN AW-5083)	4.29 wt%	0.1 wt%
AlZn5 (EN AW-7075)	2.83 wt%	5.7 wt%

For the estimation of interaction time of the melt with the laser beam the welding process is observed by high speed cameras and the capillary length and width are measured. Fig. 1 (a) shows an image from a high-speed video of the vapor capillary. The average melt flow velocity around the capillary is calculated by equation (1) from Beck, 1996 and Bronstein et al., 2008 using the capillary width and the melt pool width.

$$v_{S,AVE} = \frac{2}{\pi} * v_V \left(2 * \frac{b_S}{b_S - b_D} - 1\right) \quad (1)$$

$v_{S,AVE}$: average melt flow velocity; v_V: feed rate; b_S: width of melt pool; b_D: width of vapor capillary

The element content of the weld is determined by WDX measurement at 3 points in each weld seam at the top, in the center and at the root. The positions are shown in Fig. 1 (b). For one parameter 3 weld seams are measured and the results are averaged.

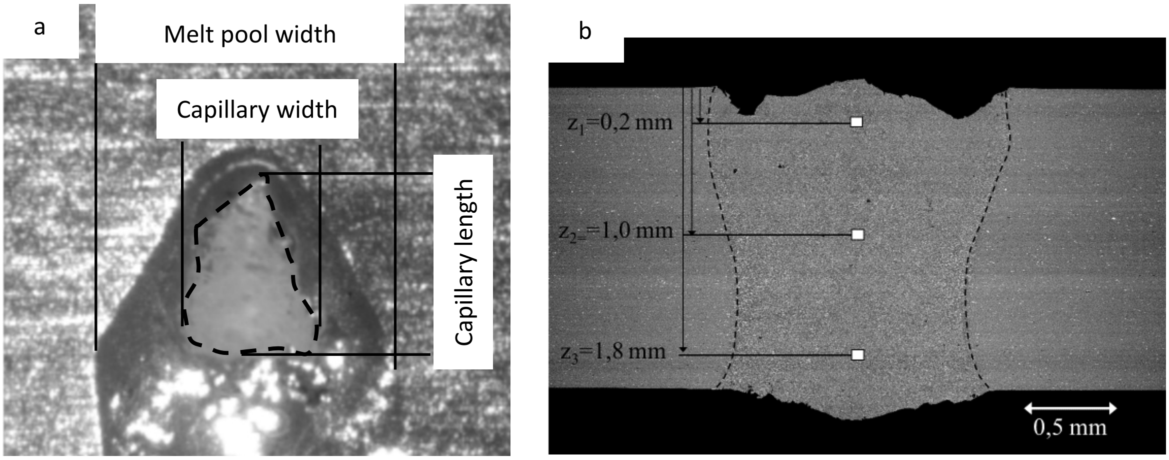

Fig. 1. (a) Image from a high-speed camera to measure geometrical features; (b) position of WDX measurement

3. Diffusion model of element loss

The volatile elements are transported from the base material to the surface of the vapor capillary by diffusion. The diffusion can be either molecular or turbulent. The element content in the melt pool can be calculated using equation (2) (Baehr and Stephan, 2013).

$$\frac{w_0 - w}{w_0 - w_{KO}} = \mathrm{erfc}\frac{x}{2\sqrt{D * t_W}} \tag{2}$$

w_0: element content of base metal; w: element content; w_{KO}: element content at capillary surface; erfc: complementary error function; x: distance from surface; D: diffusion coefficient; t_W: interaction time

The content of volatile elements at the capillary surface is unknown. Numerical simulations have shown the concentration at the surface is w = 0 kg/kg (Klassen, 2018) after an interaction time of t_W = 4 µs. Furthermore, the diffusion coefficient D is unknown. The self-diffusion in aluminum at evaporation temperature is estimated to $D = 4*10^{-8}\ m^2/s$ (Lu et al., 2006). Nevertheless, if turbulent diffusion is involved, the diffusion coefficient can be much higher (Baehr and Stephan, 2013).

In Fig. 2 (b) the element content dependent on the distance to the capillary surface is given for different diffusion coefficients D. The diagram can be interpreted as a cross section through the melt pool from the surface of the capillary to the fusion zone (Fig. 2 (a)). When the melt flows around the capillary, alloying elements are evaporated at the surface and transported from the fusion line towards the capillary surface by diffusion. The higher the diffusion coefficient, the larger is the depleted zone for a given interaction time t_W. Increasing the interaction time at a given diffusion coefficient, also enlarges the depleted zone. This is shown in Fig. 2 (c).

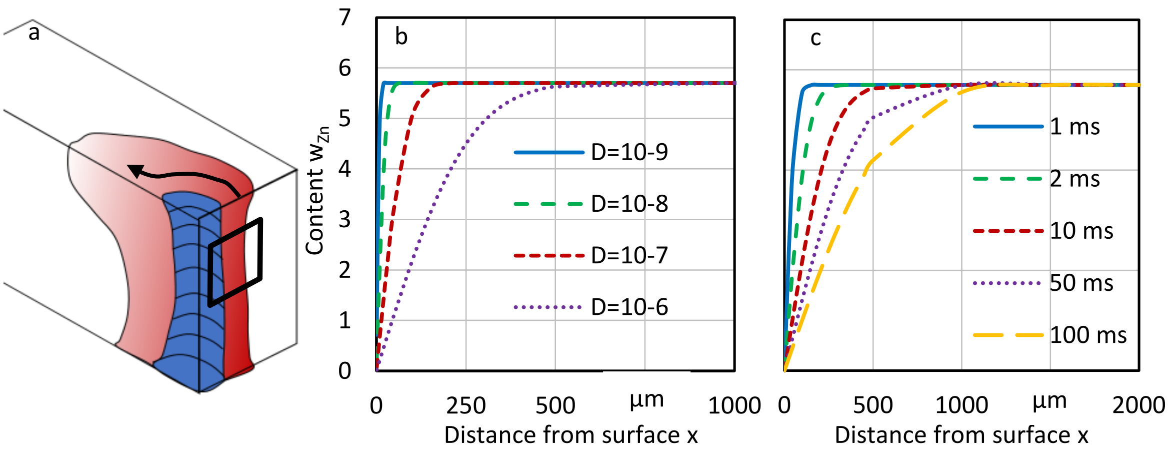

Fig. 2. Element content as a function of distance from capillary surface for AlZn5 (a) Cross section through the melt pool; (b) w_0=5,7 wt%; w_{KO}=0 wt%; t_W=20 ms; (c) D=1*10^{-6} m^2/s; $w_{0,Zn}$=5.7 wt%; $w_{KO,Zn}$=0 wt%.

The local element content in the melt pool can be integrated over the melt pool width to calculate the total element loss Δw. An example is given in Fig. 3 (a) as a function of interaction time. A longer interaction time increases the total element loss. The interaction time can be translated into an average melt flow velocity as shown in Fig. 3 (b).

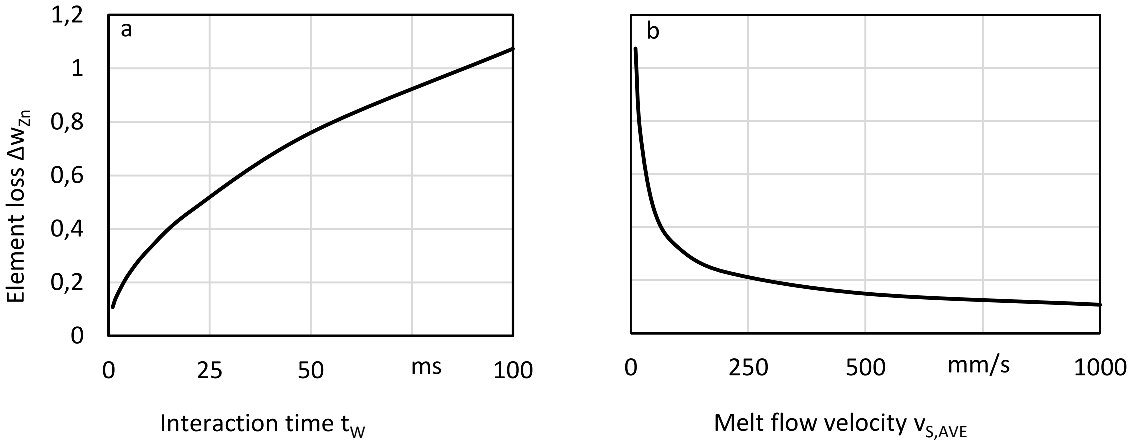

Fig. 3. (a) Element loss as a function of interaction time; (b) Element loss as a function of average melt flow velocity, D=1*10^{-6} m^2/s; $w_{0,Zn}$=5,7 m%; $w_{KO,Zn}$=0 m%; b_S=2 mm; d_F=160 µm

Moreover, the mass flow rate of the volatile element can be calculated using equation (3) (Baehr und Stephan 2013). At the surface at x = 0 µm the mass flow rate is equal to the evaporation rate.

$$k_i = \frac{\sqrt{D}}{\sqrt{\pi * t_W}} (\beta_0 - \beta_{KO}) * \exp\left(-\frac{x^2}{4 * D * t_W}\right) \quad (3)$$

k_i: evaporation rate; β_0: element concentration of base metal; β_{KO}: element concentration at capillary surface; x: distance from surface; D: diffusion coefficient; t_W: interaction time

The element concentration is calculated from element content by equation (4).

$$\beta_i = w_i * \rho_{BM} \quad (4)$$

β_i: element concentration; w_i: element content; ρ_{BM}: density of base metals

The calculation results of the evaporation rate are given in Fig. 4 for all investigated alloys as a function of interaction time of the laser beam with the melt. The parameters used for the calculation are given in the label of the picture.

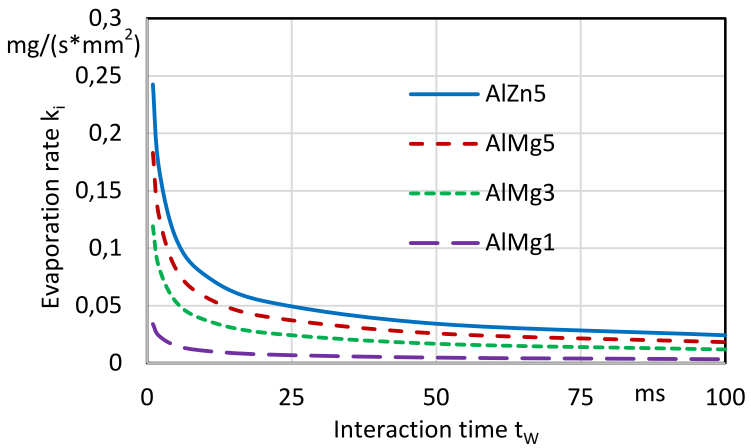

Fig. 4. Evaporation rate as a function of interaction time for different aluminum alloys, $D=10^{-8}\,m^2/s$; $\beta_{0,AlZn5}=136\ kg/m^3$; $\beta_{0,AlMg5}=103\ kg/m^3$; $\beta_{0,AlMg3}=67\ kg/m^3$; $\beta_{0,AlMg1}=19\ kg/m^3$; $\beta_{KO,Zn}=0\ kg/m^3$

In the calculations the diffusion coefficient and the surface element concentration are unknown. As only one of them can be identified from equation (3), the surface concentration is estimated as $x = 0\ kg/m^3$ and the diffusion coefficient will be determined from experiments. In the following section some results for the influence of process parameters on element loss are presented. Subsequently the evaporation rate k_i of volatile elements for different alloys is determined. From a comparison of experimental and calculation results the diffusion coefficient can be deduced.

4. Experimental results

Fig. 5 (a) shows the absolute element loss as a function of feed rate for different laser power for the alloy AlZn5. The element loss is decreasing with increasing feed rate and increasing with higher laser power. In Fig. 5 (b) the dependency of element loss from focal diameter is displayed. With increasing focal diameter, the element loss is also increasing.

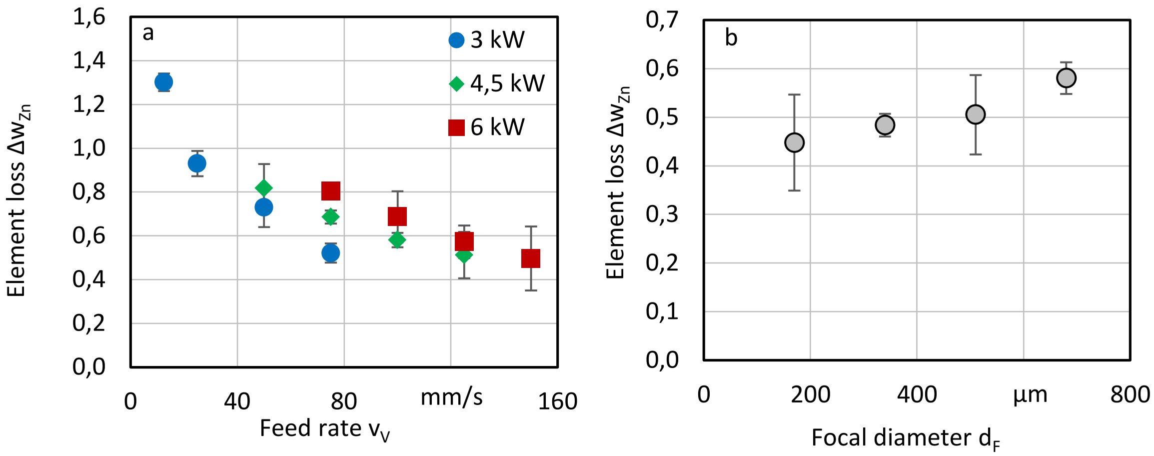

Fig. 5. (a) Element loss as a function of interaction time, AlZn5; d_f=680 µm; (b) Element loss as a function of average melt flow velocity, AlZn5; v_V=100 mm/s; P_L=4,5 kW

Since the size of the capillary, the weld pool with and the weld seam width are different for each parameter set the element loss at different parameters cannot be compared. Therefore the element loss is translated into an evaporation rate using measuring results. The element loss per area is calculated by equation (5).

$$\Delta w_{i,A} = b_N * s_B * \Delta w_i \quad (5)$$

$\Delta w_{i,A}$: element loss of a weld seam area; b_N: weld seam width; s_B: sheet thickness; Δw_i: element loss

From this result the element loss per unit weld seam length is derived using equation (6).

$$\Delta m_{i,L} = b_N * s_B * \Delta\beta_i = \Delta w_{i,A} * \rho_{BE} \quad (6)$$

$\Delta m_{i,L}$: element loss per unit length; b_N: weld seam width; s_B: sheet thickness; $\Delta\beta_i$: element loss as element concentration [kg/m^3]; Δw_i: element loss [wt%]; ρ_{BE}: density of base metal

Subsequently the total evaporation rate K_i is calculated by equation (7).

$$K_i = \Delta m_{L,i} * v_V \quad (7)$$

K_i: total evaporation rate [mg/s]; $\Delta m_{i,L}$: element loss per unit length; v_V: feed rate

Finally, the evaporation rate per unit area of the capillary surface results from equation (8). The perimeter of the capillary U_D can be measured from high-speed images.

$$k_i = \frac{K_i}{U_D * s_B * \pi} = \frac{\Delta m_{L,i} * v_V}{U_D * s_B * \pi} \quad (8)$$

k_i: evaporation rate [mg/(s*mm^2]; $\Delta m_{i,L}$: element loss per unit length; U_D: perimeter of capillary; s_B: sheet thickness; v_V:

feed rate

The interaction time of the laser beam with the melt is given by equation (9). The average melt flow velocity is calculated using equation (1).

$$t_W = \frac{U_D * \pi}{2 * v_{S,AVE}} \quad (9)$$

t_W: interaction time; U_D: perimeter of capillary; $v_{S,AVE}$: average melt flow velocity

Fig 6. shows the transformed results from Fig. 5. The element loss is translated into an evaporation rate and the feed rate is transformed into an interaction time.

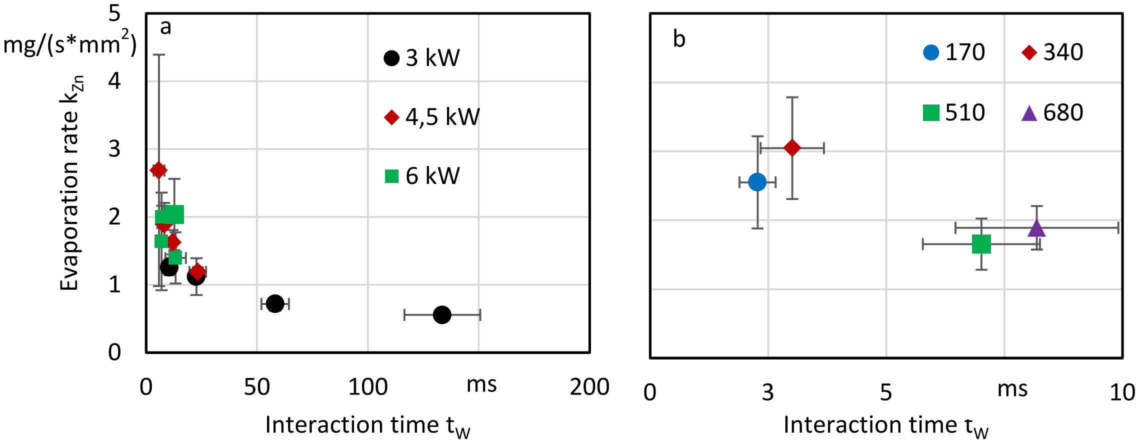

Fig. 6. (a) Evaporation rate as a function of interaction time for different laser powers, AlZn5; d_F=680 µm; (b) Evaporation rate as a function of interaction time for different focal diameters, AlZn5; v_V=100 mm/s; P_L=4,5 kW

In order to determine a pattern, Fig. 7 shows the results of a wide parameter range of laser power, feed rate and focal diameter for the alloy AlZn5. The data points are grouped to different line energies. It can be observed that the evaporation rate is an inverse function of the interaction time as estimated with the diffusion model. The calculations match the experimental results when the diffusion coefficient is set to $D_{AlZn5}=4*10^{-6}$ m^2/s. This means that the diffusion coefficient is much higher than previously assumed and the diffusion process is based on turbulent transport.

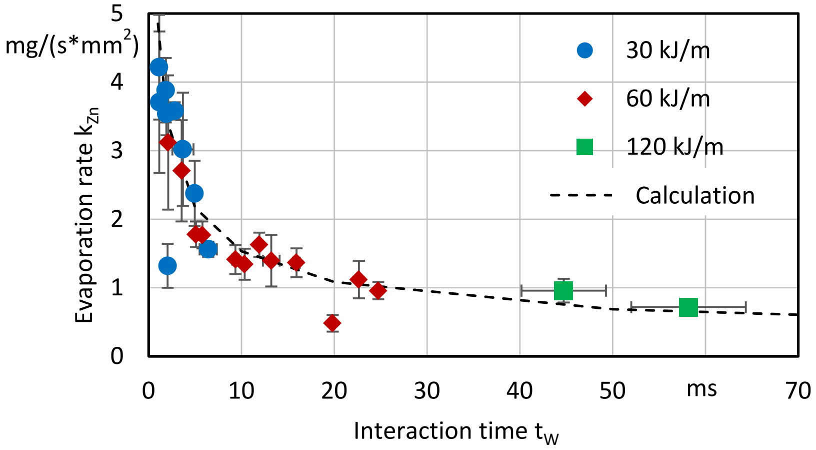

Fig. 7. Element loss as a function of interaction time for AlZn5, D=4*10^{-6} m^2/s.

As shown in Fig. 8, similar results are derived for the other alloys. Nevertheless, in order to match the experimental results, the diffusion coefficient must be adapted for each alloy: D_{AlMg1}=9*10^{-6} m^2/s, D_{AlMg3}=4*10^{-6} m^2/s and D_{AlMg5}=6*10^{-6} m^2/s.

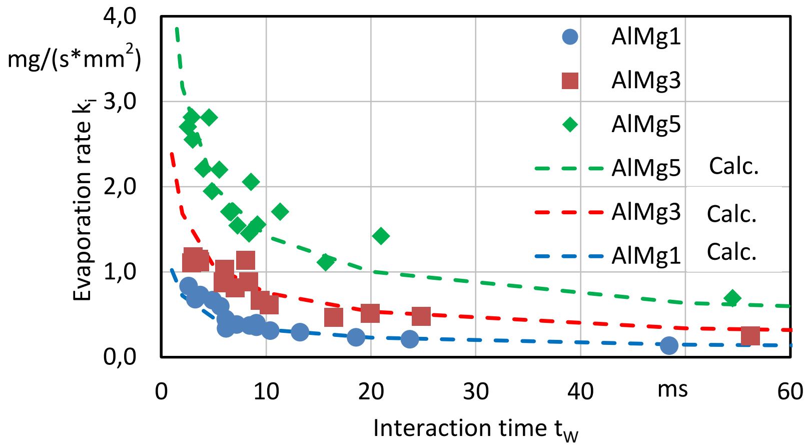

Fig. 8. Element loss as a function of interaction time for AlMg1, AlMg3 and AlMg5.

5. Summary

A simple diffusion model is employed to calculate the evaporation rate for the laser welding process of different aluminum alloys. The surface concentration of volatile elements and the diffusion coefficient are unknown. The surface concentration is set to $\beta = 0$ kg/m^3 and the diffusion coefficient is calculated by comparing experimental results to calculations. The calculations match the experimental results when the diffusion coefficient is in the range 4*10^{-6} m^2/s<D<9*10^{-6} m^2/s depending on the alloy.

References

Baehr, H. D., Stephan, K., 2013. Wärme- und Stoffübertragung. Springer, Berlin, Heidelberg.

Beck, M., 1996. Modellierung des Lasertiefschweißens. University of Stuttgart.

Bronstein, I. N., Semendjajaew, K. A., Musiol, G., Mühlig, H., 2008. Taschenbuch der Mathematik. Wisenschaftlicher Verlag Harri Deutsch, Frankfurt am Main.

Collur, M. M., Paul, A., Debroy, T., 1987. Mechanism of alloying element vaporazation during laser welding, MTB 18 (4), p. 733.

Dilthey, U., Goumeniouk, A., Lopota, V., Turichin, G., Valdaitseva, E., 2001. Development of a theory for alloying losses during laser beam welding, J. Phys. D: Appl. Phys. 34, p. 81.

Jandaghi, M., Parvin, P., Tokamany, M. J., Sabbaghzadeh, J., 2009. Measurement of the composition change in Al5754 alloy during long pulsed Nd:YAG laser welding based on LIBS, J. Phys. D: Appl. Phys. 42.

Khan, P. A. A., Debroy, T., David, S. A., 1988. Laser beam welding of high-manganese stainless stells. Examination of alloying element loss and microstructural changes, Welding Journal.

Klassen, A., 2018. Simulation of evaporation phenomena in selective electron beam melting. FAU, Erlangen.

Liu, T., Ynag, L. J., Wie, H. L., Qiu, W. C., Debroy, T., 2017. Composition change of stainless steels during keyhole mode laser welding, Welding Journal (96), p. 258.

Lu, H. M., Li, G., Zhu, Y. F., Jiang, Q., 2006. Temperature dependence of self-diffusion in several liquid metals, Journal of Non-crystalline solids 352 (26-27), p. 2797.

Mundra, K., Debroy, T., 1993. Towards understanding alloying element vaporazation during laser beam welding of stainless steel, Welding Journal.